4.6 Ground-based Retrieval of Seasonal Cloud and Precipitation Properties in the Arctic

Chuanfeng Zhao*[1], Tim Garrett[1]

University of Utah, Salt Lake City, Utah

1 Introduction

Clouds and precipitation play an important role in the energy and moisture budget of the Arctic region (Curry et al. 1996). While their properties are difficult to determine from space because the underlying snow/ice surface has little visible, thermal or microwave contrast with clouds, ground-based retrievals can be obtained from the Department of Energy (DOE) Atmospheric Remote Sensing Measurement (ARM) program North Slope of Alaska (NSA) site near Barrow, Alaska. Here, a new set of retrieval techniques suited to NSA are described, from which seasonal variability of low-level Arctic clouds and precipitation are obtained.

2 Retrieval Algorithm

2.1 Precipitation retrieval

ARM Doppler radar velocity and reflectivity are used to obtain precipitation properties. Precipitation is assumed to be present when laser determined cloud base H_{base} is higher than radar determined cloud base H_{radar} by 45 m, where 45 m is half of the radar range gate. Precipitation phase is assumed to be ice when temperature at precipitation level (T_p) is below 273.15 K, and water when T_p is above 273.15 K.

The precipitation particle terminal velocity V_T is related to its particle spherical radius r_{sphere} (Gelbard et al. 1980; Heymsfield 1972) through

$$V_T = K_1 r_{sphere}^2 / f, \quad r_{sphere} < 40\,\mu\mathrm{m} \tag{1}$$

$$V_T = K_2 r_{sphere} / f, \quad 40\,\mu\mathrm{m} < r_{sphere} < 0.6\,\mathrm{mm} \tag{2}$$

where f is a shape factor, $K_1 = 1.19 \times 10^6\,\mathrm{cm}^{-1}\mathrm{s}^{-1}$ and $K_2 = 8 \times 10^3\,\mathrm{s}^{-1}$ are empirical parameters, and r_{sphere} is the radius of a spherical droplet with a mass equivalent to the precipitation particle. It is assumed that $f = 1$ for liquid droplet and $f = 4$ for column ice particles (Heymsfield 1972; Ohtake et al. 1982).

Here, we assume that the mean terminal velocity $\overline{V_T}$ and log-normal mode radius r_n of precipitation are equivalent to V_T and r_{sphere}, respectively. Frisch et al. (2002) argued that averaged over several minutes, the measurements of radar Doppler velocity of precipitation $< V_D >$ approach the mean precipitation particle velocity $\overline{\omega}$. Assuming further that ω and V_T are similar because the Arctic is generally stable with low updraft speeds relative to V_T, the precipitation mode radius r_n can be obtained from $< V_D >$ according to

$$r_n = (< V_D > f/K_1)^{1/2} \quad r < 40\,\mu\mathrm{m} \tag{3}$$

$$r_n = < V_D > f/K_2 \quad 40\,\mu\mathrm{m} < r < 0.6\,\mathrm{mm} \tag{4}$$

Assuming a log-normal size distribution for precipitation (Frisch et al. 1995),

$$r_{eP} = r_n exp(2.5 ln^2 \sigma_g) \tag{5}$$

$$N_P = Z/(2^6 r_n^6 exp(18 ln^2 \sigma_g)) \tag{6}$$

$$P_P = \frac{4}{3}\pi \rho_i V_T r_{eP}^3 N_P / \rho_w \tag{7}$$

where Z is the radar reflectivity, r_{eP} and N_P are the effective radius and number concentration of the precipitation, P_P is the precipitation rate, ρ_i and ρ_w are the bulk density of ice and water, respectively, and σ_g is the assumed standard deviation of a log-normal size distribution.

2.2 Cloud retrieval

To obtain the cloud properties of single-layer stratus in the Arctic, we have modified an ice cloud retrieval

* *Corresponding author address:* Chuanfeng Zhao, 135 S 1460 E, Room 819 Salt Lake City, UT 84112-0110; e-mail: czhao@met.utah.edu

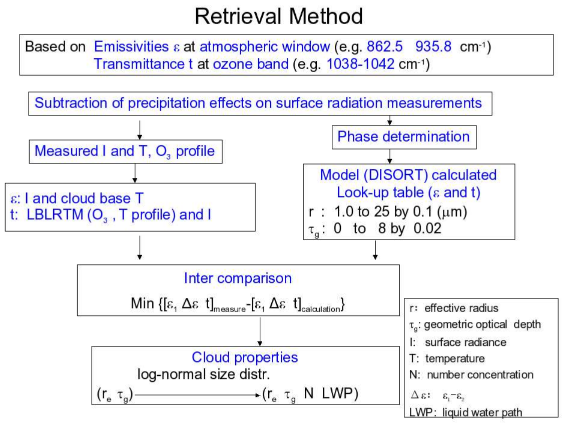

Figure 1: Single-layer thin cloud retrieval method.

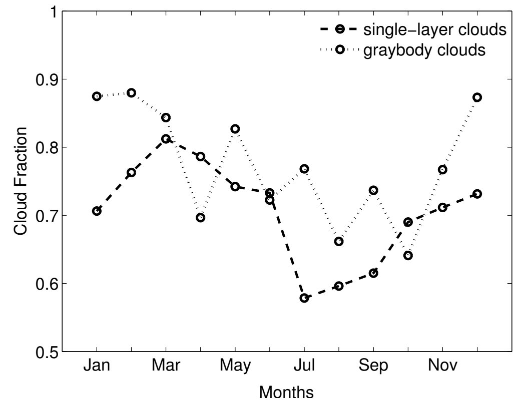

Figure 2: The fraction of clouds which are single-layer, and the fraction of single-layer clouds which are graybodies.

algorithm developed by Mahesh et al. (2001) for application to the Antarctic. The retrieval method requires ARM NSA-AAO ground-based remote sensing measurements, and Global Ozone Monitoring (GOME) stratospheric ozone profile measurements from the European Remote Sensing (ERS-2) satellite.

As illustrated in Fig. 1, the retrieval method consists of six parts: 1) subtraction of precipitation effects on surface downwelling infrared radiation, 2) determination of cloud phase, 3) selection of emissivity (ε) microwindows at which ε varies monotonically with cloud effective radius (r_e) and geometric optical depth (τ_g), 4) calculation of a look-up table for emissivity (ε) and transmittance (t_c) as a function of r_e and τ_g, 5) calculation of ε and t_c based on measurements, and 6) retrieval of r_e and τ_g through a minimization process based on an intercomparison between calculated ε, t_c and those from the look-up table.

This retrieval algorithm is similar to Mahesh et al. (2001) with the exception that it includes the subtraction of precipitation radiance, that cloud phase is determined based on the cloud emissivity between 800 and 900 cm^{-1} (Turner et al. 2003) and the cloud brightness at 8.4 $\mu\mathrm{m}$ and 10.7 $\mu\mathrm{m}$ (King et al. 2004), and that cloud base is determined using laser instead of the CO_2- slicing method.

Cloud water path (WP) and particle number concentration (N) can be computed from

$$WP = 2\rho r_e \tau_g / 3 \quad (8)$$
$$N = 3WPexp(3.0\sigma^2)/(4\pi\rho r_e^3 \Delta H) \quad (9)$$

where ρ is bulk density, σ is the standard deviation for cloud particle size distribution, and ΔH ($H_{top} - H_{base}$) is the cloud depth.

We should note that this retrieval method is applicable only to single-layer graybody clouds. Fig. 2 shows the values of monthly fraction of clouds which are single-layer, and the fraction of single-layer clouds which are graybodies. In each month, over 60% of clouds are single-layer, and over 65% single-layer clouds are graybodies. Even 90% of single-layer clouds are graybodies in winter. However, the fraction of clouds which are graybodies ranges from 40% in summer to 60% in winter. Thus, the cloud properties retrieved with our method are just for part, not all of the Arctic clouds, and the retrieved cloud liquid water path will be low biased.

3 Results

Fig. 3a shows retrieved ice crystal precipitation (ICP) properties between 2000 and 2003. ICP effective radius (r_{eICP}) and number concentration (N_{ICP}) median values are 0.052 l^{-1} and 226 $\mu\mathrm{m}$, respectively, with a standard deviation of 64.6 l^{-1} and 130 $\mu\mathrm{m}$, respectively. For comparison, Ohtake et al. (1982) observed Arctic column ice crystals with size range of 30-300 $\mu\mathrm{m}$ on the c-axis and 15-25 $\mu\mathrm{m}$ on the a-axis at low temperatures. Girard and Blanchet (2001) described Arctic diamond dust with particle number concentrations less than 4 cm^{-3}.

Fig. 3b, c and d show monthly distributions of precipitation effective radius (r_{eP}), number concentration (N_P) and precipitation rate (P_P) between 2000 and 2003. Precipitation effective radius r_{eP} increases during spring and decreases during fall, and precipitation number concentration N_P is nearly uniform in spring and decreases in fall, indicating reduced precipitation in winter. r_{eP} is a minimum

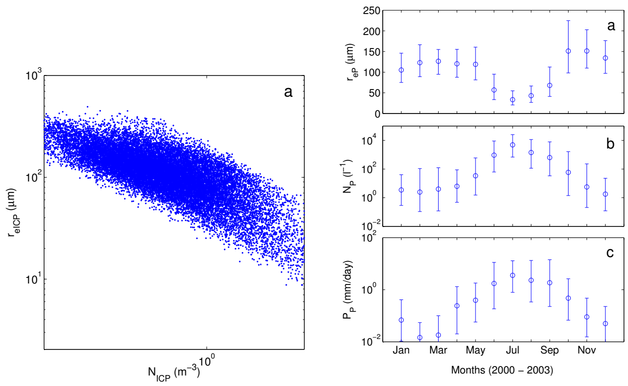

Figure 3: The properties of retrieved precipitation. (a) the range of retrieved ice crystal precipitation effective radius (r_{eICP}) and number concentration (N_{ICP}) values. (b, c and d) the monthly distributions for median values of precipitation effective radius (r_{eP}), number concentration (N_P) and precipitation rate (P_p).

(30~50 $\mu\mathrm{m}$) and N_P is a maximum (1~10 cm^{-3}) in summer, which may be caused by precipitation liquid phase and sufficient water sources from ocean. The monthly mean precipitation rate increases in spring and reaches a maximum (3.57 $\mathrm{mm/day}$) in July, and it decreases in fall and reaches a minimum (0.01 $\mathrm{mm/day}$) in February. The annual mean values for r_{eP}, N_P, and P_P are about 107 $\mu\mathrm{m}$, 393 l^{-1} and 0.88 $\mathrm{mm/day}$, respectively.

Estimates of cloud phase indicate that most low-level thin clouds are liquid clouds in all seasons, but especially so in summer. Ice and mixed-phase clouds form mainly in winter, when their incidence is about 40% and 4%, respectively (Fig. 4a). Fig. 4b, c and d show the properties of liquid clouds. Liquid cloud particle effective radius r_e ranges from 2 to 25 $\mu\mathrm{m}$, and cloud number concentration N ranges from 3 cm^{-3} to 300 cm^{-3}. The annual mean values of retrieved r_e and N are 10.1 $\mu\mathrm{m}$ and 112 cm^{-3}, respectively. Clouds are thinnest in winter, although retrievals are limited to gray-body clouds with LWP generally less than 150 $\mathrm{g\,m}^{-2}$ Cloud number concentration N decreases about 80 cm^{-3} and effective radius r_e increases about 4 $\mu\mathrm{m}$ between winter and summer. Garrett and Zhao (2006) have shown these changes can be attributed to Arctic haze events from mid-latitude pollution sources, which are common during winter and spring.

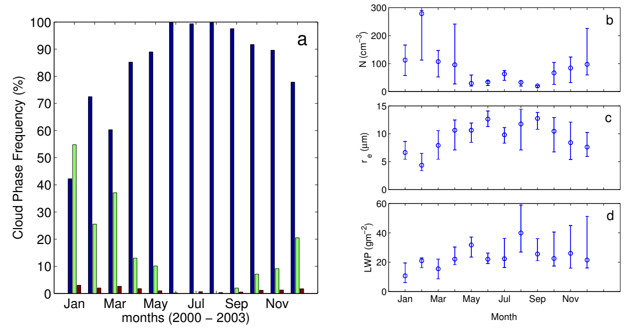

Figure 4: (a) monthly distribution of water (blue), ice (green) and mixed-phase (brown) clouds between 2000 and 2003. (b, c and d) monthly mean cloud properties (r_e, N and LWP).

4 Bibliography

Curry, J. A., W. B. Rossow, D. Randall and J. L. Schramm, 1996: Overview of Arctic cloud and radiation characteristics. *J. Climate*, **9**, 1731-1764.

Frisch, A. S., Fairall, C. W., Snider, J. B.. 1995: Measurement of stratus cloud and drizzle parameters in ASTEX with a K_α-band Doppler radar and a microwave radiometer. *J. Atmos. Sci.*, **52**, 2788-2799.

Frisch, A. S., and M. D. Shupe, 2002: Stratus cloud drizzle retrieval during SHEBA from MMCR Doppler moments. *Twelfth ARM science team meeting proceedings, St. Petersburg, Florida, April 8-12*.

Garrett, T. J., C. Zhao, 2006: Increased Arctic cloud longwave emissivity associated with pollution from mid-latitudes. *Nature*, **440**, 787-789.

Gelbard, F., Y. Tambour, and J. H. Seinfeld, 1980: Sectional representation for simulating aerosol dynamics. *J. Colloid Interface Sci.,* **76**, 541-556.

Girard, E., and J. P. Blanchet, 2001:Microphysical parameterization of Arctic diamond dust, ice fog, and thin stratus for climate models. *J. Atmos. Sci.*, **58**, 1181-1198.

Heymsfield, A., 1972: Ice crystal terminal velocities. *J. Atmos. Sci.*, **29**, 1348-1357.

King, M. D., S. Platnick, P. Yang, G. T. Arnold, M. A. Gray, J. C. Riedi, S. A. Ackerman and K. N. Liou, 2004: Remote sensing of liquid water and ice cloud optical thickness and effective radius in the Arctic: Application of airborne multispectral MAS data. *J. Atmos. Ocean. Tech.*, **21**, 857-875.

Mahesh, A., V. P. Walden, and S. G. Warren, 2001:

Ground-based infrared remote sensing of cloud properties over the Antarctic plateau. Part II: cloud optical depths and particle sizes. *J. Appl. Meteor.*, **40**, 1279-1294.

Ohtake, T., Jayaweera, K. O. L. F. and Sakurai, K. I. 1982: Observation of ice crystal formation in lower Arctic atmosphere. *J. Atmos. Sci.*, **30**, 2898-2904.

Turner, D. D., S. A. Ackerman, B. A. Baum, H. E. Revercomb, and P. Yang, 2003: Cloud phase determination using ground-based AERI observations at SHEBA. *J. Appl. Meteor.*, **42**, 701-715.